

# Entrapment of Nickel in Ferrochrome Ash by Native *Lysinibacillus sp* Bacteria

**Mahindra Kothuri, Devatha CP**  
National Institute of Technology Karnataka  
Srinivasanagar, Surathkal, India

mahindrakothuri.187cv006@nitk.edu.in; devathafce@nitk.edu.in

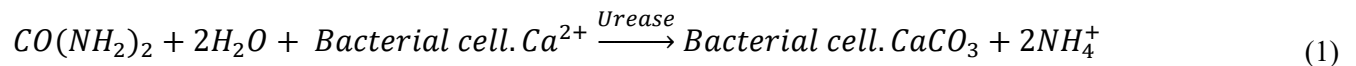
**Abstract** – Nickel contamination in water is a significant environmental concern and causes several health effects such as allergies, cardiovascular diseases, and cancers in human beings. Ferrochrome ash is a fine dust generated as the waste from steel industry and pollutes the flow-through water by leaching nickel present in it. By providing a pre-disposal treatment of microbial induced calcite precipitation (MICP) to ferrochrome ash, the nickel leaching can be substantially reduced. Bacteria secrete the urease enzyme that decides the rate of urea hydrolysis reaction and they are the nucleation sites for the precipitation of calcium carbonate in calcium rich environment. During MICP, calcium carbonate entraps the nickel present in the ash. As a result, the nickel cannot escape the ash matrix and hence do not pollute the contacting water. This was confirmed by the atomic absorption spectrophotometric analysis (AAS) on leachates from treated and untreated ash. The analysis resulted in less nickel content from treated ash with highest treatment efficiency of 98% at LS 100. Results from SEM, FTIR, XRD, and TG implied that calcium carbonate developed in the ash due to MICP.

**Keywords:** Ferrochrome ash, urea hydrolysis, nickel entrapment, *Lysinibacillus sp*, leaching

## 1. Introduction

Ferrochrome ash is the fine dust generated from gas cleaning chambers in ferrochromium industry. It is more dangerous than the ferrochrome slag, due to the presence of high concentrations of heavy metals prone to leaching [1]. Nickel is one of the toxic heavy metals in ferrochrome ash. It is a critical contaminant and causes harmful effects on human health like allergies, cardiovascular and kidney diseases, lung fibrosis, and nasal cancer [2]. It contaminates the contact water through leaching mechanism. Hence, it is not safe to dispose ferrochrome ash in open dump sites. It is always better to prevent contamination than to treat the polluted water. Therefore, it is necessary to prevent water contamination with a sustainable mechanism that is based on ecofriendly, cost-effective materials and methods.

Calcium carbonate is a non-reactive and inert material generated by the reaction between calcium and carbonates formed during urea hydrolysis [3]. Urea hydrolysis is controlled by an enzyme named urease, secreted by specific bacteria. Carbonates react with the calcium ions located on the bacterial surfaces and precipitate dense layers of calcium carbonate around the bacteria. The process of developing calcium carbonate by bacteria is collectively known as microbially induced calcite precipitation (MICP).



MICP has been successfully used for soil strengthening, ground water remediation, and plugging of geological formations [4]. However, MICP has not been used as a waste treatment technology to dictate the concentration of leachate. The objective of the present study is to reduce the nickel content in leachates from ferrochrome ash. Since nickel is a cation like calcium, it is also co-precipitated during MICP along with calcium carbonate. The treated ferrochrome ash is analyzed using XRD, FTIR, SEM and TG for detecting the changes in the ash due to MICP.

## 2. Materials and Methods

Ferrochrome ash used in this study contained 555 mg of nickel in the form of NiO per 1 kilogram of ferrochrome ash. Stoichiometrically, it is equivalent to 436 mg of Ni<sup>2+</sup> (Table 1). Urea and calcium oxide used in this study were laboratory grade from MERCK.

Table 1: Elemental composition of ferrochrome ash.

Oxide composition	Weight %
Fe <sub>2</sub> O <sub>3</sub>	3.83%
SiO <sub>2</sub>	16.4%
Al <sub>2</sub> O <sub>3</sub>	7.69%
MgO	22.5%
Na <sub>2</sub> O	2.19%
K <sub>2</sub> O	14.20%
NiO	0.56%

### 2.1. Bacteria

Ferrochrome ash dispersed in a sterile nutrient broth medium contained the native bacteria and the bacterial density spiked by incubation at 37°C for 10 hours in an orbital shaker at 150 rpm. Urease producing bacteria isolated using Christensen's agar for identification by 16SrRNA analysis.

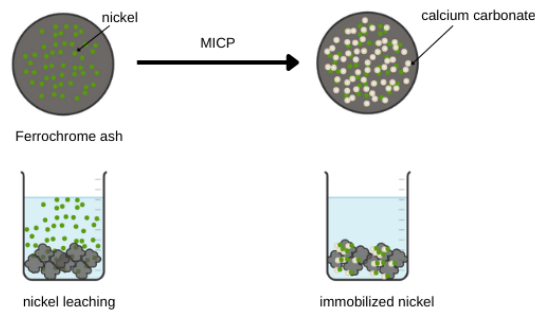


Fig. 1: Nickel leaching reduced by MICP

### 2.2. MICP Treatment

Ferrochrome ash blended with 0.05 molar urea and calcium oxide along with the enhanced bacteria for the MICP treatment. Treated ferrochrome ash was dispersed in distilled water at liquid-solid (LS) ratios 10, 25, 50 and 100 and mixed well for 18 hours at 30rpm followed by vacuum filtration through 0.45µm filter and stored at 4°C before analyzing for nickel content.

### 2.3. Leachate Analysis

Aliquots were estimated for nickel concentration by atomic absorption spectrophotometer (Systronics). Light beam of 230nm wavelength determines the nickel content in the liquid. The efficiency of nickel fixation evaluated as the percentage of nickel concentration changed in the leachates from mineralized and untreated ash as shown in equation 2. AAS analysis of the leachates denotes the efficiency of MICP in nickel entrapment.

$$Efficiency \% = \frac{(L_1 - L_2)}{L_1} \times 100 \quad (2)$$

Where,  $L_1$  and  $L_2$  are the nickel concentrations in leachates of untreated and treated ferrochrome ash respectively.

## 2.4. Characterization Studies

Changes developed in ferrochrome ash by MICP treatment was observed by X-ray diffraction, Fourier transform infrared spectroscopy, scanning electron microscopy and thermogravimetric analyses.

## 3. Results

### 3.1. Native Bacteria

*Lysinibacillus Sp* was the urease producing bacteria in ferrochrome ash identified using 16S rRNA sequence analysis. A phylogenetic tree was constructed by the Neighbor-joining method (Figure 2). The genetic data was submitted to NCBI GenBank with accession number OM346720. The bacteria were grown in a liquid broth medium with the composition of soybean, yeast extract, and glucose. The optical density of the bacterial medium was 1.58 at 600nm measured by a UV-visible spectrophotometer (Systronics). Bacteria had urease activity of 27.83 m.mol urease/min estimated by the electrical conductivity method [5]. The initial pH of bacterial media was 6.25 and it increased to 8.96 during the MICP treatment.

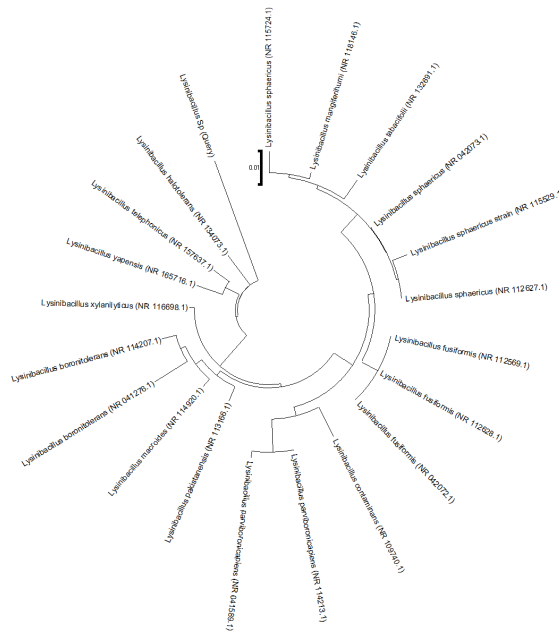


Fig. 2: Phylogenetic tree of native *Lysinibacillus Sp.* in ferrochrome ash

### 3.2. Treatment Efficiency

As observed from the figure 3, the nickel content in leachate from the treated ferrochrome ash was less than untreated ash at all the LS ratios. At LS 10, the nickel concentration was 41.64 ppm and 3.522 ppm in the leachates from ferrochrome ash before and after the MICP treatment, respectively. In the same order, the concentrations of nickel were 16.95 ppm and 1.186 ppm for LS25, 8.58 ppm and 0.403 ppm for LS50 and 4.42 ppm and 0.106 ppm for LS100. Highest efficiency of 98% the MICP treatment

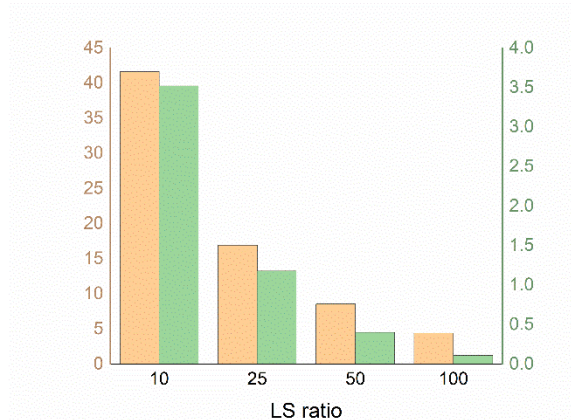


Fig. 3: Nickel concentration in leachates from ferrochrome ash before (orange) and after (green) the MICP treatment in ppm.

### 3.3. Fourier Transform Infrared Spectroscopy

Treated ferrochrome ash analyzed by the KBr method on the FTIR spectrometer (Jasco FTIR 4200) between 4000 and 400 $\text{cm}^{-1}$  developed the characteristic infrared spectrum (Figure 4). The absorption band at 712  $\text{cm}^{-1}$  represents the in-plane deformation caused by the OCO bending and the absorption band at 873  $\text{cm}^{-1}$  corresponds to inadequate plane deformation of  $\text{CO}_3$  [6]–[8]. The peaks at 1159 $\text{cm}^{-1}$  and 1448  $\text{cm}^{-1}$  correspond to the stretching vibration of CO [9]. The observed peaks over 3000 $\text{cm}^{-1}$  were due to the combined effect of NH stretching and OH stretching.

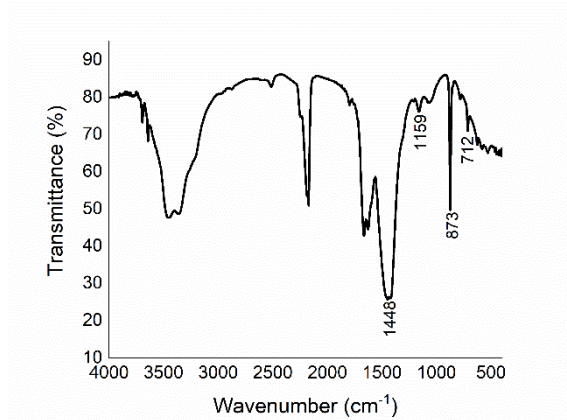


Fig. 4: IR spectrum of treated ferrochrome ash

### 3.4. X-Ray Diffraction

The crystalline phase of the mineral was identified by the X-ray diffraction study. The precipitate formed during mineralization was analyzed on the diffractometer (EMPYREAN PAN analytical) from 10 to 80° 2 $\theta$  with Cu-K $\alpha$  1.54. The raw diffraction data was processed in X'pert Highscore Plus software aided by the ICSD database. The predominant components were identified as calcite and portlandite (Figure 5). 73% of the precipitate contained calcite and the rest was portlandite. The highest intensity peaks of calcite and portlandite were detected at diffraction angles of 29.434° and 34.130°, respectively. In the precipitate, calcite was the result of urea hydrolysis in the presence of calcium and portlandite occurred due to the reaction of calcium oxide with water.

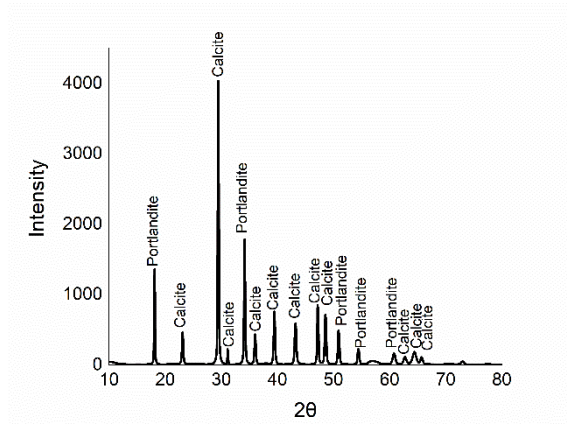


Fig. 5: Mineral composition of treated ferrochrome ash

### 3.5. Thermogravimetric Analysis

Biomaterial thermograph (Figure 6) in the nitrogen atmosphere from the 25 to 825° C temperature range was recorded using the thermogravimetric analyzer (Seiko Exstar TG-DTA 6300). Weight loss was observed in three temperature regions. The weight loss in the sample at a temperature of less than 200° C was the loss of interparticle water. At about 400° C, the loss was due to the decomposition of portlandite. A further weight reduction between 580° C and 670° C was due to the calcite decomposition. Similar observations of weight loss due to the decomposition of  $\text{Ca}(\text{OH})_2$  and  $\text{CaCO}_3$  was observed in earlier studies [10]–[12].

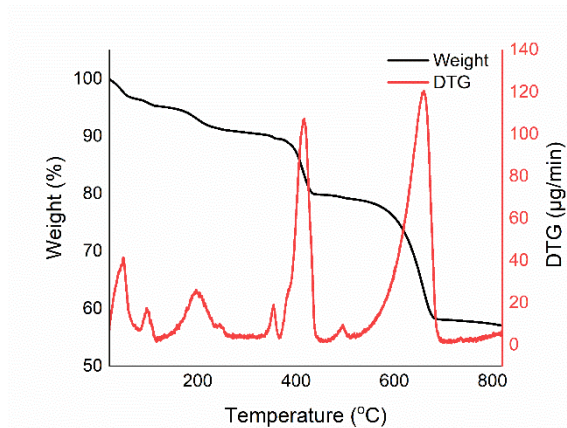


Fig. 6: Thermal behavior of the treated ferrochrome ash

### 3.6. Scanning Electron Microscopy

The microstructure of the ferrochrome ash before and after MICP was examined using the scanning electron microscope (ZEISS GeminiSEM 300). Ferrochrome ash contained fine particles with many void spaces among them (Figure 7a). Whereas, in treated ferrochrome ash, the ash particles were surrounded by the calcium carbonate. Hence, the particles appear densely packed, and the free space was occupied by the calcium carbonate formed during MICP (Figure 7b). The observation made with the XRD analysis that the biomaterial composition contained calcite and portlandite was evident by the SEM images.

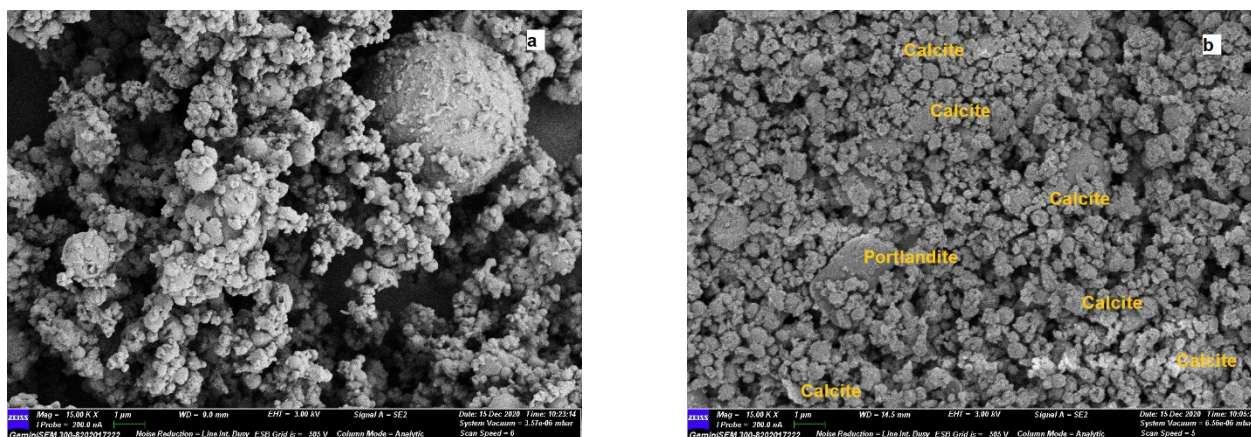


Fig. 7: Surface morphology of ferrochrome ash (a) before MICP treatment and (b) after MICP treatment

#### 4. Discussion

The present study was aimed at reducing the nickel content in leachate from ferrochrome ash. To achieve it, ferrochrome ash was treated with MICP. Bacteria isolated from the ferrochrome ash and the culture grown on Christensen's agar was used for urea hydrolysis. Native bacteria were preferred over known bacterial strains because the indigenous bacteria naturally have immunity against toxic heavy metals in the ash and they do not need to newly acclimatize to the environment in the ash. The bacteria identified as *Lysinibacillus Sp* and was grown in a nutrient medium with a composition of soybean, yeast extract powder and glucose. The composition with relatively inexpensive materials was suitable for multiplying bacteria with excellent growth and urease activity. The bacterial medium was added to the ferrochrome ash and blended with urea and calcium oxide for the MICP treatment.

The pH was increased due to the formation of carbonate ions in the medium indicating the mineralization. Results from XRD, FTIR, SEM and TG analyses identified the formed precipitate as calcite and portlandite. Calcite formed as the result of MICP and the portlandite was the result of the hydrolysis of calcium oxide. The leachate analysis indicated that biomineralization could fix nearly 98% of leachable nickel in the ash. When analyzing leachates at different L-S ratios, it was understood that nickel was trapped by calcite and the formed precipitates were stable under different solubility conditions.

Nickel immobilization ensures that the ferrochrome ash do not pollute the water contacting the ferrochrome ash due to the formation of a non-reactive layer of calcium carbonate encapsulates the nickel ions. They obstruct the movement of nickel from the ferrochrome ash to the contact water. Thus, objective of the present study to reduce the nickel contamination of leachates from ferrochrome ash has been achieved by the co-precipitation of nickel with calcium carbonate by the MICP treatment.

#### 5. Conclusion

The results of this investigation show that *Lysinibacillus Sp*, a native bacterium from ferrochrome ash can restrict nickel leaching. Coprecipitation with calcium carbonate controlled the leaching of nickel in ferrochrome ash efficiently at different LS ratios with a least efficiency of 92% at LS10 and highest efficiency of 98% at LS 100. FTIR, XRD, SEM, and TG analyses recognized the major change happened in the ferrochrome ash due to MICP was the formation of calcite and portlandite. From the results of this study, it can be concluded that native bacteria have a natural tendency to remediate the ferrochrome ash when provided with conditions suitable for urea hydrolysis.

#### Acknowledgements

The authors are thankful to the Ministry of Education, Govt. of India, for providing fellowship to Mr. Kothuri Mahindra to pursue his research studies at NITK-Surathkal. The authors are grateful to the Department of Chemical

Engineering, Department of Metallurgical and Materials Engineering, and Central Research Facility of NITK-Surathkal for providing the laboratory facilities.

## References

- [1] G. Kiely, *Environmental Engineering*. Chennai: McGraw Hill Education (India) Private Limited, 2017.
- [2] G. Genchi, A. Carocci, G. Lauria, M. S. Sinicropi, and A. Catalano, "Nickel: Human health and environmental toxicology," *International Journal of Environmental Research and Public Health*, vol. 17, no. 3. MDPI AG, Feb. 01, 2020. doi: 10.3390/ijerph17030679.
- [3] A. Rajasekar, S. Wilkinson, and C. K. S. Moy, "MICP as a potential sustainable technique to treat or entrap contaminants in the natural environment: A review," *Environmental Science and Ecotechnology*, vol. 6, Apr. 2021, doi: 10.1016/j.ese.2021.100096.
- [4] B. Krajewska, "Urease-aided calcium carbonate mineralization for engineering applications: A review," *Journal of Advanced Research*. 2018. doi: 10.1016/j.jare.2017.10.009.
- [5] N. Jalilvand, A. Akhgar, H. A. Alikhani, H. A. Rahmani, and F. Rejali, "Removal of Heavy Metals Zinc, Lead, and Cadmium by Biomineralization of Urease-Producing Bacteria Isolated from Iranian Mine Calcareous Soils," *J Soil Sci Plant Nutr*, vol. 20, no. 1, pp. 206–219, 2020, doi: 10.1007/s42729-019-00121-z.
- [6] F. B. Reig, J. V. G. Adelantado, and M. C. M. Moya Moreno, "FTIR quantitative analysis of calcium carbonate (calcite) and silica (quartz) mixtures using the constant ratio method. Application to geological samples," *Talanta*, vol. 58, no. 4, pp. 811–821, Oct. 2002, doi: 10.1016/S0039-9140(02)00372-7.
- [7] N. v. Vagenas, A. Gatsouli, and C. G. Kontoyannis, "Quantitative analysis of synthetic calcium carbonate polymorphs using FT-IR spectroscopy," *Talanta*, vol. 59, no. 4, pp. 831–836, Mar. 2003, doi: 10.1016/S0039-9140(02)00638-0.
- [8] M. Sharma, N. Satyam, and K. R. Reddy, "Investigation of various gram-positive bacteria for MICP in Narmada Sand, India," *International Journal of Geotechnical Engineering*, vol. 15, no. 2, pp. 220–234, 2021, doi: 10.1080/19386362.2019.1691322.
- [9] A. Śliwińska, A. Smolinski, and P. Kucharski, "Simultaneous analysis of heavy metal concentration in soil samples," *Applied Sciences (Switzerland)*, vol. 9, no. 21, Nov. 2019, doi: 10.3390/app9214705.
- [10] Z. Mirghiasi, F. Bakhtiari, E. Darezereshki, and E. Esmaeilzadeh, "Preparation and characterization of CaO nanoparticles from Ca(OH)<sub>2</sub> by direct thermal decomposition method," *Journal of Industrial and Engineering Chemistry*, vol. 20, no. 1, pp. 113–117, Jan. 2014, doi: 10.1016/j.jiec.2013.04.018.
- [11] K. Weise, N. Ukrainczyk, and E. Koenders, "A mass balance approach for thermogravimetric analysis in pozzolanic reactivity r3 test and effect of drying methods," *Materials*, vol. 14, no. 19, Oct. 2021, doi: 10.3390/ma14195859.
- [12] T. Kim and J. Olek, "Effects of sample preparation and interpretation of thermogravimetric curves on calcium hydroxide in hydrated pastes and mortars," *Transp Res Rec*, no. 2290, pp. 10–18, 2012, doi: 10.3141/2290-02.